A Letters Journal Exploring the Frontiers of Physics

January 2014

EPL, **105** (2014) 27004
doi: 10.1209/0295-5075/105/27004

www.epljournal.org

Domain walls in helical magnets: Elasticity and pinning

T. Nattermann

Institut für Theoretische Physik, Universität zu Köln - Zülpicher Str. 77, D-50937 Köln, Germany

received 22 November 2013; accepted in final form 9 January 2014
published online 7 February 2014

PACS 75.10.-b – General theory and models of magnetic ordering
PACS 75.60.-d – Domain effects, magnetization curves, and hysteresis
PACS 75.70.Kw – Domain structure (including magnetic bubbles and vortices)

Abstract – Recently completely new types of domain walls (DWs) have been discovered in helical magnets, consisting generically of a regular array of *pairs* of magnetic vortex lines (Li F. *et al.*, *Phys. Rev. Lett.*, **108** (2012) 107203). Only for special orientations DWs are free of vortices. In this paper we calculate their elastic and pinning properties, using the pitch angle θ as a small parameter. In particular we show that vortex-free DWs exhibit long-range elasticity which makes them very stiff and suppresses their pinning by impurities. Their roughening transition temperature is of the order of the Néel temperature. DWs including vortices (either by orientation or due to step formation above their roughening transition) show short-range elasticity and strong pinning by impurities. These results apply both to centrosymmetric as well as to non-centrosymmetric systems. The application to chiral liquid crystals is briefly discussed.

Introduction. – Pinning plays a key role in condensed-matter systems: it restores the state of zero resistance in type-II superconductors by anchoring flux lines, it hardens steel by blocking the motion of dislocations [1], but, in contrast, prevents charge density waves to become ideal conductors [2]. In ferroelectrics and ferromagnets pinning of domain walls influences their coercivity and switching behavior [3,4], strongly relevant for potential applications as storage media [5]. In all cases pinning and hysteresis result from the competition of the impurity potential, which favors deformations of the condensed structure, and the rigidity of the latter, which penalizes them. The appearance of a non-zero coercive force requires the emergence of multistability of the resulting effective potential landscape [6].

Recently a new type of magnetic DWs —different from Bloch or Néel walls— has been predicted for helical magnets [7]. Helical magnets are abundant, occurring as metals and alloys [8–12], semiconductors [13] and multiferroics [14–21]. The latter group is most interesting for applications [15]. It was shown in [7] that for almost all orientations DWs in these systems consist of a regular array of magnetic vortex lines. These walls can be driven by currents and, in multiferroics, by electric fields [7]. Vortex walls have indeed be seen in circularly polarized X-rays in Ho [9], and by Lorentz-TEM in FeGe [12]. Only for special orientations DWs are vortex free. Special cases of the latter have been studied previously by Hubert [3] and will called in this paper *Hubert walls* (see fig. 1).

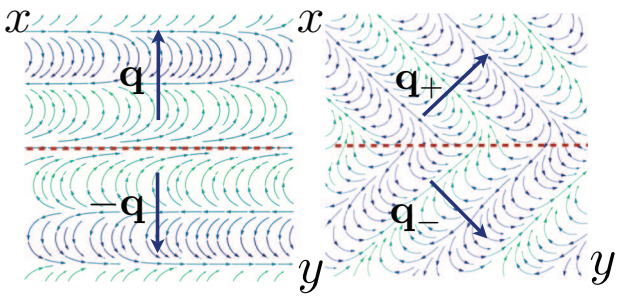

Fig. 1: (Colour on-line) Cross-section of Hubert walls in helical magnets. Left panel: centrosymmetric system, right panel: non-centrosymmetric system. The small arrows denote the orientation of **m**, the large arrows the wave vectors **q**. For systems where $\mathbf{m}\cdot\hat{x} = 0$, **m** has been rotated by $\pi/2$ around y for better visibility.

Outline and results. – In the present letter I investigate the elasticity and impurity pinning of DWs in helical magnets. I show that their micro-magnetic model can be considerably simplified by writing it in a form similar to the London theory of superconductors. In this description

magnetic vortices result from a fictitious magnetic field acting only inside the DW. Vortex-free Hubert walls are found to exhibit *non-local* elasticity which makes them too stiff to be pinned by impurities. Hence they can easily disappear from the sample, which may explain why Hubert walls were not observed so far in experiment [22]. Roughening of Hubert walls occurs by entropy or disorder-driven proliferation of steps. Steps consist of pairs of vortex lines of the same vorticity which *attract* each other. The roughening transition temperature T_R is calculated and found to be of the order of the Néel temperature. Additional disorder-driven roughening of Hubert walls is shown to have a weak effect only.

On the contrary, DWs including vortices exhibit local elasticity and are strongly pinned by disorder. I also discuss the effect of weak anisotropy on Hubert walls. Although most of the derivations are presented for centrosymmetric systems, it is shown that the results transfer to the non-centrosymmetric case as well. Finally I discuss some conclusions for DWs in chiral liquid crystals.

Hamiltonian. – To describe helical magnets I use the appropriate micro-magnetic Hamiltonian $\mathcal{H}[\mathbf{m}(\mathbf{r})]$. $\mathbf{m} = (m_x, m_y, 0)$ denotes the magnetization, assuming $m_z = 0$. Since in helical magnets both time and space inversion symmetry are broken, their paraphase can be either *centrosymmetric* or *non-centrosymmetric*.

Centrosymmetry requires invariance with respect to space and time inversion, *i.e.* $\mathbf{r} \to -\mathbf{r}$ and $\mathbf{m} \to -\mathbf{m}$. If there are only two modulation vectors, $\mathbf{q} = \pm(\theta/a)\hat{x}$, as in most centrosymmetric systems, one finds up to quadratic terms in $\mathbf{m}$ [3]

$$\mathcal{H} = \frac{J}{2}\int_{\mathbf{r}}\left[-\frac{\theta^2}{2a}(\partial_x\mathbf{m})^2 + \frac{a}{4}(\partial_x^2\mathbf{m})^2 + \frac{1}{a}(\nabla_\perp\mathbf{m})^2\right]. \quad (1)$$

Here $\int_{\mathbf{r}} = \int \mathrm{d}^3r$ and $\nabla_\perp = \hat{y}\partial_y + \hat{z}\partial_z$. θ and a denote the angle between adjacent spins along the x-direction and the lattice constant, respectively. The continuum approach is valid provided $\theta \ll \pi$. Experimentally one finds $\theta \approx 0.27$–0.73 under ambient conditions [8] and $\theta \to 0$ under uniaxial pressure [23]. In systems where indirect RKKY exchange between $4f$ electrons [24] results in nearest-neighbor ferromagnetic ($J > 0$) and next-nearest-neighbor anti-ferromagnetic ($J' < 0$) interaction, $\theta = \arccos(J/4|J'|)$ in the ground state [3]. With the replacement $m_x + im_y = e^{i\phi}$ Hamiltonian (1) can be written as

$$\mathcal{H} = \frac{Ja}{8}\int_{\mathbf{r}}\left\{\left[(\partial_x\phi)^2 - q^2\right]^2 + \frac{4}{a^2}(\partial_\perp\phi)^2 + \left(\partial_x^2\phi\right)^2\right\}. \quad (2)$$

Non-local elasticity of Hubert walls. – Calculation of pinning forces requires the knowledge of the elasticity of DWs [6]. It is convenient to introduce a rotated coordinate system with one axis, say ξ, parallel to the (average) normal $\hat{n}$ of the DW and the two other axes, $(\eta, z) \equiv \boldsymbol{\eta}$, perpendicular to $\hat{n}$, *i.e.* parallel to the DW plane. Since the system is isotropic in the yz-plane, it is indeed sufficient to restrict the normal $\hat{n}$ to the xy-plane. Rotation of $\hat{n}$ around the x-axis does not change the results. Thus we define

$$\xi = x\cos\alpha + y\sin\alpha, \quad \eta = -x\sin\alpha + y\cos\alpha \quad (3)$$

with α the angle between the x-axis and $\hat{n}$. The energy of long wavelength elastic DW distortions $u(\boldsymbol{\eta})$ from a planar reference configuration then reads

$$\mathcal{H}_{el} = \tfrac{1}{2}\int \mathrm{d}\boldsymbol{\eta}\mathrm{d}\boldsymbol{\eta}'\mathcal{G}^{-1}(\boldsymbol{\eta} - \boldsymbol{\eta}')u(\boldsymbol{\eta})u(\boldsymbol{\eta}'). \quad (4)$$

We begin with the Hubert wall where $\alpha = 0$, $\xi = x, \eta = y$ and hence $\boldsymbol{\eta} = (y, z)$. To determine $\mathcal{G}(\boldsymbol{\eta})$ I assume that the DW distortions are of *buckling* type, *i.e.* free of vortices (but see below). The saddle point solution for the undistorted Hubert wall is known exactly [3]

$$\phi_0(x, x_0) = \ln\cosh[q(x - x_0)]. \quad (5)$$

To find the corresponding solution for the distorted wall is more cumbersome since (2) includes the quartic term $\left[(\partial_x\phi)^2 - q^2\right]^2$. Instead I will resort to an approximation and replace this term by $4q^2\left[\partial_x\phi - A(\mathbf{r})\right]^2$. $A(\mathbf{r})$ is assumed to be constant inside a domain ($A = \pm q$) and to change smoothly from $-q$ to q on a scale q^{-1} when crossing the DW. With this replacement the resulting quadratic Hamiltonian resembles the London theory of type-II superconductors

$$\mathcal{H}_0 = \tfrac{1}{2}Ja\int_{\mathbf{r}}\left[\theta^2\left(\partial_x\phi - A\right)^2 + (\partial_\perp\phi)^2 + \frac{a^2}{4}\left(\partial_x^2\phi\right)^2\right]. \quad (6)$$

$\mathbf{A} = (A, 0, 0)$ plays the role of a vector potential which generates a fictive magnetic field $\mathbf{B} = \nabla \times \mathbf{A}$ acting only inside the DW. The linear saddle point equation corresponding to (6) and the non-linear saddle point equation corresponding to (2) have identical solutions, provided $A(\mathbf{r})$ and $\phi(\mathbf{r})$ obey the relation

$$\partial_x A = \tfrac{3}{2}\left[1 - (\partial_x\phi/q)^2\right]\partial_x^2\phi. \quad (7)$$

For a planar Hubert wall we get from (5), (7)

$$A(x) = q\tanh(qx)\left[1 + \cosh(qx)^{-2}\right] \quad (8)$$

which exhibits the expected smooth behavior of A. The solution for a *distorted* Hubert wall is conveniently calculated from the saddle point equation of (6) by an Ansatz invented by Joanny and de Gennes in the context of contact lines [25]

$$\phi(\mathbf{r}) = \int_0^x \mathrm{d}x' A(x') + \int_{\mathbf{k}} e^{i(k_y y + k_z z) - |\mathbf{k}||x|/\theta}\alpha_{\mathbf{k}}. \quad (9)$$

Here $\int_{\mathbf{k}} = \int \mathrm{d}k_y\mathrm{d}k_z/(2\pi)^2$. The first term describes the unperturbed phase field, the second term its corrections up

to a distance $|\mathbf{k}|^{-1}$ from the average wall position. Moreover we ignored the last term in (6) which is justified for $k \ll q\theta$. $\alpha_{\mathbf{k}}$ is to be determined from the condition

$$\phi\left[u(\boldsymbol{\eta}), \boldsymbol{\eta}\right] = 0. \tag{10}$$

To lowest order in u, one finds $\alpha_{\mathbf{k}} = -u_{\mathbf{k}} q$, provided $|\mathbf{k}| < q\theta$. Plugging (9) back into the quadratic Hamiltonian one obtains for the Fourier transform of $\mathcal{G}(\boldsymbol{\eta})$

$$\hat{\mathcal{G}}_H^{-1}(\mathbf{k}) \approx J|q|^3 \left(4|\mathbf{k}| + a\mathbf{k}^2/3\right). \tag{11}$$

Equation (11) is valid for distortions $|qu| > 1$. The dominant term $\sim |\mathbf{k}|$ results from the long-range self-interaction of the DW which a makes it very stiff. The second term in (11) is the contribution from the increased surface area due to the wall distortion and is relevant only for large $\mathbf{k}$. In real space the energy expression (11) for the Hubert wall is *non-local*, $\mathcal{G}_H^{-1}(\mathbf{r}) \sim J(|q|/|\mathbf{r}|)^3$, in contrast to Bloch and Néel walls, whose elasticity is strictly local. As we will see this has dramatic consequences for the pinning of Hubert walls since a strictly planar wall is not pinned.

Roughening transition of Hubert walls. – Next I consider the possibility of a roughening transition [26] of the Hubert wall which would render elasticity short-ranged [27]. A roughening transition occurs due to the formation and proliferation of terraces, separated by steps, on the Hubert wall (see fig. 2). Steps can occur due to thermal fluctuations or disorder. To study step formation more in detail I consider a Hubert wall with a step at $y = 0$, parallel to the z-axis. The cross-section of a step is shown in the left panel of fig. 2. The phase ϕ across the step can be described by the function

$$\phi_s(x, y) \equiv \phi_0\left(x - \tau\pi/q\right) + \tau\pi \mathrm{sign}\left(x - \tau\pi/q\right) \tag{12}$$

where $\tau = \mathrm{sign} y$ and $\phi_0(x)$ is given in (5). $\phi_s(x, y)$ is smooth across $y = 0$ for $|x| \gg \pi/q$. On the contrary, in the region $|x| < \pi/q$ the sign of $\partial_x \phi_s$ is opposite for $y \lessgtr 0$. Hence the integral along a contour $\mathcal{C}$ inclosing the step gives $\oint_{\mathcal{C}} \phi = 4\pi$, *i.e.* the step consists of *two* vortices. In this construction the vortex configuration was restricted to a narrow slice of width a. The step energy per unit length, ε_s, is of the order $J/(a\theta)$. Further relaxation of the configuration ϕ_s by allowing the vortex to extend over a larger region can only *decrease* ε_s. The step consists of two nearby vortices of the same vorticity. Each of them fulfils the approximate saddle point equation

$$-a^2 \partial_x^4 \phi_s + 4\partial_\perp^2 \phi_s = 0, \tag{13}$$

following from (2) provided the distance from the vortex centre is less than $2\pi/q$. An approximate solution of (13) is given by the Ansatz

$$\phi(x > 0, y) = \arcsin\left[y/(\kappa^2 x^4 + y^2)^{1/2}\right]. \tag{14}$$

κ is a variational parameter. With $x^2 = ra\cos\varphi/\kappa$, $y = r\sin\varphi$, (14) gives for the vortex energy density $J\mathcal{E}_v(x, y)$

$$\mathcal{E}_v(x, y) \approx \frac{1}{2ar^2}\left[\cos^2\varphi + \kappa^2 \sin^2\varphi (1 - 4\cos^2\varphi)^2\right]. \tag{15}$$

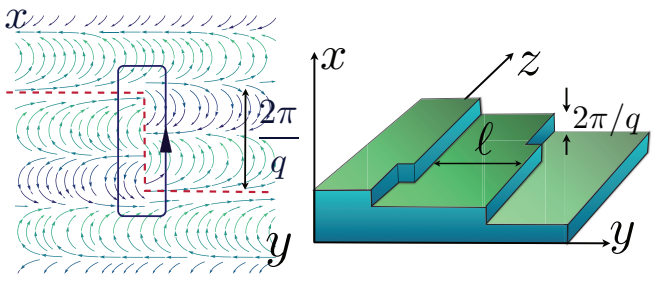

Fig. 2: (Colour on-line) Left panel: cross-section of a Hubert walls with a step before relaxation. The arrows denote again the orientation of $\mathbf{m}$. The step extends perpendicular to the picture plane. The contour $\mathcal{C}$ encloses two vortices. Right panel: vortex wall consisting of an array of steps separated by terraces of Hubert walls.

Minimization gives for the vortex core energy per unit length $E_v \approx 0.6J/a$, $\kappa = 0.42$ [28] and hence $\varepsilon_s \approx 1.2J/a$. The two vortices attract each other with a force proportional to the length of the vortex line. Using the step energy ε_s in the results for the roughening transition in the ASOS model [29] one obtains for the roughening transition temperature of the Hubert wall $T_R^{(H)} \approx J/k_B$. Adopting for the Néel temperature T_N the result for the 3D XY-model (corresponding to the use of (6)) one finds $T_N \approx 2.2J/k_B$ [30]. This approximation is restricted to a region not too close to the Lifshitz point $\theta = 0$. Above T_R the Hubert wall exhibits short-range elasticity. However, since T_R is of the order T_N, the non-local elasticity dominates over a large temperature region.

I have also studied the possibility of *disorder-driven* roughening of Hubert walls which would render its elasticity local [31]. Using arguments similar to those used in [32] I found that the effective step energy surrounding a terrace of linear size L vanishes on scales $L > a\exp[1/(|\theta|^7 c_{\mathrm{imp}})]$. Here

$$c_{\mathrm{imp}} = n_{\mathrm{imp}} v_0^2/a^3 \tag{16}$$

is a dimensional expression for the strength of collective pinning. n_{imp} and v_0 denote the impurity concentration and volume, respectively. Hence terraces *are* generated spontaneously by the disorder. Because of the exponentially large length scale this effect will hardly be seen and hence Hubert walls remain flat and elasticity non-local as long as $T < T_R$.

Elasticity of vortex walls. – Next I consider a DW whose normal is tilted away by an angle α from the x-axis. Such a wall includes vortices. It consists of steps considered in the previous section which are separated by terraces of average width $\ell = 2\pi a/(\theta \tan\alpha)$ (see fig. 2, right panel). The surface energy $\sigma(\alpha)$ of the DW can then be written as

$$\sigma(\alpha) \approx \left[\sigma_H + \varepsilon_{\mathrm{int}}(\ell)\right] |\cos\alpha| + \sigma_v |\sin\alpha|. \tag{17}$$

$\sigma_H = J\theta^3/(3a^2)$ and $\sigma_v = \varepsilon_s\theta/(2\pi a)$ are the surface tension of the Hubert ($\alpha = 0$) and the pure vortex wall ($\alpha = \pi/2$), respectively. $\varepsilon_{\rm int}(\ell)$ describes the step interaction. At $T = 0$, $\varepsilon_{\rm int}(\ell) \approx \sigma_v \exp(-q\ell)$, whereas at $T > 0$ $\varepsilon_{\rm int}(\ell) \sim T/\ell^2$ due to collisions of meandering steps [27]. To obtain the elastic constants of the DW one has to consider an infinitesimal homogeneous distortion $\partial_\eta u \equiv \epsilon$ away from the plane perpendicular to the DW normal $\hat{n}$ [26]. This changes the surface energy density by

$$\frac{\sigma(\alpha+\epsilon)}{\cos\epsilon} - \sigma(\alpha) \approx \sigma'(\alpha)\epsilon + \frac{1}{2}\left[\sigma(\alpha) + \sigma''(\alpha)\right]\epsilon^2. \quad (18)$$

The linear term in ϵ vanishes at finite temperatures since the roughening transition temperature for the vicinal surface considered here vanishes. This follows from the fact that Hubert walls are structureless in the plane orthogonal to $\hat{x}$ and hence steps can meander freely, leading to a rough surface [27]. A distortion $\partial_z u$ leads to a similar expression without derivative terms since the $\sigma(\alpha)$ depends only on α. The total elastic energy for the vortex wall can therefore be written as

$$\hat{\mathcal{G}}_v^{-1}(\mathbf{k}) = \gamma(\alpha)k_\eta^2 + \sigma(\alpha)k_z^2, \quad (19)$$

i.e. vortex walls exhibit conventional elasticity. Note that

$$\gamma(\alpha) = \sigma(\alpha) + \sigma''(\alpha) = \varepsilon''_{\rm int}\cos\alpha - 2\varepsilon'_{\rm int}\sin\alpha \quad (20)$$

only depends on the vortex interaction which is small for small α. Here $\varepsilon'_{\rm int} = d\varepsilon'_{\rm int}[\ell(\alpha)]/d\alpha$ etc.

A corresponding calculation for $\alpha \approx \pi/2$ is more difficult. The height h of steps in pure vortex walls can take any value, but steps cannot meander freely since vortex walls have a structure periodic in the $\hat{x}$-direction. However, the step energy is small in this case since vortices can almost freely slide against each other and hence $T_R \ll J/k_B$.

DW pinning by impurities. – DWs can be pinned by impurities [1]. The statistical pinning theory of DWs with local elasticity has been developed some time ago [33]. In the present context it will be applied to Hubert and vortex walls. I assume the presence of non-magnetic impurities which dilute the system and hence contribute a term

$$\mathcal{H}_{\rm imp} = -J\int_{\mathbf{r}} \delta\tau(\mathbf{r})\mathcal{E}[\boldsymbol{\eta}, u(\boldsymbol{\eta}) - \xi] \quad (21)$$

to its energy. Here $J\mathcal{E}$ is the energy density of the domain wall and $\delta\tau = v_0\sum_i \delta(\mathbf{r}-\mathbf{r}_i)$ where $\mathbf{r}_i$ denotes the impurity position. We will assume that $v_0^{1/3}q \ll 1$ such that the pinning energy correlation length parallel to ξ is of the order of the DW width $\sim q^{-1}$. The local pinning force density $f(\eta, u)$ follows then from

$$f = -\frac{\delta\mathcal{H}_{\rm imp}}{\delta u(\boldsymbol{\eta})} = \sum\nolimits_i J^2 v_0\delta(\boldsymbol{\eta} - \boldsymbol{\eta}_i)\mathcal{E}'(\boldsymbol{\eta}, u - \xi_i), \quad (22)$$

where $\mathcal{E}'(\boldsymbol{\eta}, u-\xi_i) = \mathrm{d}\mathcal{E}(\boldsymbol{\eta}, u-\xi_i)/\mathrm{d}u$. Averaging over the random $\mathbf{r}_i$ one obtains $\langle f\rangle = 0$ and

$$\langle f(\boldsymbol{\eta}, u)f(\boldsymbol{\eta}', u')\rangle = \delta(\boldsymbol{\eta} - \boldsymbol{\eta}')\Delta_0(\boldsymbol{\eta}, u - u'). \quad (23)$$

Here $\langle\ldots\rangle$ denotes the disorder average and

$$\Delta_0(\boldsymbol{\eta}, u) = J^2 c_{\rm imp}a^3\int \mathrm{d}\xi\mathcal{E}'(\boldsymbol{\eta}, u-\xi)\mathcal{E}'(\boldsymbol{\eta}, -\xi). \quad (24)$$

The second-order perturbation theory gives for the pinning threshold of a driven DW [33]

$$f_{\rm pin}(\boldsymbol{\eta}) = -\Delta'_0(\boldsymbol{\eta}, u \to \pm 0)\mathcal{G}(0). \quad (25)$$

Here $\pm$ sign denotes the sign of the driving force. Generically $\Delta'_0(\boldsymbol{\eta}, 0) \sim -\int \mathrm{d}\xi\{[\mathcal{E}'(\boldsymbol{\eta}, u-\xi)]^2\}' = 0$ for analytic $\Delta(u)$, since $\mathcal{E}'(x \to \pm\infty) = 0$. Then $f_{\rm pin} = 0$, *i.e.* there is *no* coercivity from perturbation theory.

A finite parameter renormalization group calculation gives a diverging coupling constant $g_l = \Delta''_l(0)$, $l = \ln(L/a)$, when approaching the (Larkin) length scale $\mathcal{L}$. The latter follows from the balance between the elastic energy $E_{\rm el}$ and the $E_{\rm pin} \sim L^{D/2}$. If $E_{\rm el} < E_{\rm pin}$, the DW can adapt to the disorder and hence acommmodate to a potential valley where it gets pinned. In the opposite case the DW is too stiff to stay in one valley. By crossing the rugged energy landscape, potential forces on the DW show either sign such that the resulting pinning force $\sim L$ and hence is surpassed by the driving force, which is typically $\sim L^2$. For systems with short-range elasticity $E_{\rm el} \sim L^{D-2}$. $D(=2)$ denotes the dimension of the domain wall. Hence $E_{\rm el} < E_{\rm pin}$ for $D < D_c = 4$ and $L > \mathcal{L}$, where $E_{\rm el}(\mathcal{L}) = E_{\rm pin}(\mathcal{L})$. Since the random potential acting on the domain wall is correlated in the ξ-direction over its width q^{-1}, the pinning force density can be estimated as

$$f_{\rm pin} \sim Jq/\mathcal{L}^2. \quad (26)$$

Pinning of Hubert walls. – As we have seen, Hubert walls exhibit non-local elasticity. Since the typical correlation length of the disorder seen by a domain wall is equal to its width $\sim q^{-1}$, it makes sense to look at the elastic energy of a distortion $u \approx q^{-1}$ on the scale L. This gives with (19) $E_{\rm el,H} \sim JLq \sim J\theta L/a$. The variance of the pinning energy $E_{\rm pin}$ is

$$\left\langle\mathcal{H}_{\rm imp}^2\right\rangle = (Jv_0)^2\sum\nolimits_i \mathcal{E}^2(\boldsymbol{\eta}_i, \xi_i) \approx (Jv_0)^2 n_{\rm imp}\int_{\xi,\boldsymbol{\eta}} \mathcal{E}^2. \quad (27)$$

The energy density of planar Hubert walls [3] is obtained from (2) and (5) as

$$\mathcal{E}_H(\boldsymbol{\eta}, \xi) \approx \frac{a}{2}\left[\phi''_0(q\xi)\right]^2 = \theta^4/\left[2a^3\cosh^4(q\xi)\right]. \quad (28)$$

We note that $\mathcal{E}_H$ depends only via u on $\boldsymbol{\eta}$ in these cases. From the last two relations we get for the Hubert wall

$$E_{{\rm pin},H}, = c_H J c_{\rm imp}^{1/2}\theta^{7/2}L/a, \quad (29)$$

where $c_H \approx 0.49$. This gives for the ratio of the pinning to the elastic energy $E_{{\rm pin},H}/E_{{\rm el},H} \sim (\theta^5 c_{\rm imp})^{1/2} \ll 1$. From this argument one does not expect any pinning of Hubert walls by impurities. However, the argument presented did

not take into account that independent pinning energy gains can be made on different length scales [32], which leads to an additional logarithmic factor $\ln(Lq)$ in the pinning energy. As a result, $E_{\mathrm{pin},H}/E_{\mathrm{el},H}$ is of order one on the exponentially large length scale

$$\mathcal{L}_H \sim q^{-1} \exp[1/(\theta^5 c_{\mathrm{imp}})^{1/2}]. \tag{30}$$

Functional renormalization group. – We will now calculate the pinning force on a Hubert wall using the functional renormalization group calculation at the critical dimension $D_c = 2$. Following the calculation scheme used in [33] one can show that the effective force correlator $\Delta_l(u)$ on scale $L = ae^l$ obeys the RG flow equation ($c = 1/(64\pi J^2 q^6)$)

$$\frac{\mathrm{d}\Delta_l(u)}{\mathrm{d}l} = c\frac{\mathrm{d}^2}{\mathrm{d}u^2}\Delta_l(u)\left[2\Delta_l(0) - \Delta_l(u)\right]. \tag{31}$$

Differentiation twice with respect to u one finds from (31), assuming $\Delta'(0) = 0$, that g obeys the equation

$$\mathrm{d}g_l/\mathrm{d}l = -6cg_l^2. \tag{32}$$

Integration with the generic initial value $g_0 < 0$ shows, that g develops a pole on scale $\mathcal{L}_H = a\exp[1/(6cg_0)]$. On larger scale $\Delta_l(u)$ exhibits a *cusp* singularity. In this region (31) can be solved with the Ansatz

$$\Delta_l(u) = c^{-1}A^2 l^{-1+2\mu}\Delta^*(uA^{-1}l^{-\mu}). \tag{33}$$

This gives for $\Delta^*(u)$ the relation

$$(1 - 2\mu - \Delta^{*\prime\prime})\Delta^* - \mu u\Delta^{*\prime} - \Delta^{*\prime 2} + \Delta^{*\prime\prime} = 0. \tag{34}$$

I have chosen A such that $\Delta^*(0) = 1$. The value $\mu = 1/3$ can be found from the fact that $\partial_l \int \mathrm{d}u\Delta_l(u) = 0$. For small u one then gets

$$\Delta^*(u) = 1 - |u|/\sqrt{3} + 2u^2/9. \tag{35}$$

Thus $\Delta^{*\prime}(\pm 0) \sim -\mathrm{sign}\, u$ and $\infty > g^* > 0$. One can now apply (25) using the *renormalized* function $\Delta_l(u)$ on scales larger $\mathcal{L}_H$. $\mathcal{L}_H$ plays the role of the short length scale cut-off of the renormalized theory. With $g_0 \approx -2.4 c_{\mathrm{imp}} J^2\theta^{11}a^{-6}$, one obtains finally for the coercive force

$$|f_{\mathrm{pin}}^{(H)}| \approx (4|\theta|/a)^3\, \pi J \exp\left[-c_p/(|\theta|^5 c_{\mathrm{imp}})\right]. \tag{36}$$

and $c_p \approx 14.2$. This result is in agreement with our previous estimate (26), (30). Since both θ, $c_{\mathrm{imp}} \ll 1$, pinning of Hubert walls by direct interaction with impurities is *completely negligible*, as long as one is below T_R. This is a direct consequence of their non-local elasticity. It implies that after a quench to a metastable multidomain state Hubert walls will quickly disappear from the sample. Indeed, in films of helical magnets with film plane perpendicular to the helical axis, domains were found to extend over the whole film width [22].

Pinning of vortex walls. – We come now to the consideration of the pining of vortex walls whose normal is tilted away from the x-direction by an angle α. Since their elasticity is short-ranged (see eq. (19)), the elastic energy of a distortion $u \sim q^{-1}$ is of the order

$$E_{\mathrm{el}} \approx q^{-2}\left[\sigma(\alpha)\gamma(\alpha)\right]^{1/2}. \tag{37}$$

To find the variance of the pinning energy of the steps (*e.g.*, in a wall where $\alpha = \pi/2$) we use the energy density expression (15) of the variational study of vortices [28] which gives for the pinning energy

$$E_{\mathrm{pin},s} \approx c_s J c_{\mathrm{imp}}^{1/2} L/a \tag{38}$$

and $c_s \approx 0.42$. The pinning energy is dominated by contributions from the centre of the vortex and hence it does not depend on θ.

We estimate the pinning energy of a wall of general orientation by

$$E_{\mathrm{pin}} \approx \left[\cos^2\alpha E_{\mathrm{pin},H}^2 + \sin^2\alpha E_{\mathrm{pin},s}^2\right]^{1/2} \tag{39}$$

$$= J c_{\mathrm{imp}}^{1/2} c_s \frac{L}{a}\sin\alpha\left[1 + (c_H\cot\alpha/c_s)^2\,\theta^7\right]^{1/2}. \tag{40}$$

Thus, as soon as $\tan\alpha > c_H\theta^{7/2}/c_s$ pinning of the domain wall is dominated by the steps. In this region the Larkin length is then given by

$$\mathcal{L}(\alpha) \sim a^3\left[\sigma(\alpha)\gamma(\alpha)\right]^{1/2}\left[J c_{\mathrm{imp}}^{1/2} c_s\theta^2\sin\alpha\right]^{-1} \tag{41}$$

and correspondingly the pinning force density (26). Note, that this result does not cross over to $\mathcal{L}_H$ since we assumed here short-range elasticity. The latter is present only on scales $L \gg \ell(\alpha)$. This result is confirmed by a functional renormalisation group calculation in $D = 4-\epsilon$ dimensions with $\epsilon = 2$ which increases the estimate of the Larkin length by a factor 70.

Anisotropy. – In systems where the $U(1)$ symmetry of the magnetic structure is broken Hubert walls are also pinned by weak anisotropy, as I will show now. It is easy to assure oneself that moving a rigid Hubert wall requires the rotation of *all* spins in at least one half-space. This rotation does not cost energy even in the presence of impurities, as long as the $U(1)$ symmetry is preserved and the interaction with impurities does not depend on the spin direction, as I assume here. Most of the experimental systems have however a weak anisotropy of the form

$$\mathcal{H}_v = -J(v/a^3)\int_{\mathbf{r}}\cos(p\phi), \quad v > 0. \tag{42}$$

For sufficiently large anisotropy helical regions of width $w = a\theta/(pv)^{1/2}$ are separated by commensurate regions of almost constant phase $\phi = 2\pi n/p$ [26]. The latter increase with increasing anisotropy until at $w < w_c \sim q^{-1}$ the system becomes ferromagnetic. Accommodation of a DW

inside a commensurate region saves energy and hence leads to pinning.

This effect works also in the case of very weak anisotropy. The ground state can then be described by a weak modulation of the wave vector

$$q(x) \approx \pm q \left\{1 - \nu \sin[pq(x - x_0)]\right\}, \quad \nu \sim v/\theta^4 \ll 1. \quad (43)$$

The absolute value of the phase gradient $q(x)$ is smallest for $pq(x_n - x_0) \approx 2\pi n, n$ integer, corresponding to the almost commensurate regions for large anisotropy. Assuming for the moment $\nu \approx 1$ ϕ_x reaches zero at $x = x_n$ for both helicities and hence a domain wall would not cost extra energy. It is clear that this effect also works for $\nu < 1$. Thus Hubert walls are pinned by the anisotropy.

Non-centrosymmetric systems. – In the generic case the Hamiltonian of non-centrosymmetric systems has the form [7]

$$\mathcal{H} = \frac{J}{2} \int_{\mathbf{r}} \left[(\nabla \mathbf{m})^2 + |\mathbf{q}| \mathbf{m}(\nabla \times \mathbf{m})\right]. \quad (44)$$

The direction of $\mathbf{q} = \theta \hat{q}/a$ is fixed by an additional weak (cubic) anisotropy of the order θ^4. θ is here proportional to the spin-orbit coupling. The anisotropy term can therefore be neglected otherwise. Hubert walls are characterized by a normal $\hat{n}$ obeying $\hat{n} \cdot \mathbf{q}_+ = \hat{n} \cdot \mathbf{q}_-$. $\mathbf{q}_+$, $\mathbf{q}_-$ are the wave vectors of the adjacent domains. To be specific I consider $\mathbf{q}_\pm = (q_x(x), q_y, 0)$ with $q_x(x)$ changing smoothly from q_x to $-q_x$ over a region of size q^{-1} when crossing the wall [7] (compare fig. 1, right panel). Expressing $\mathbf{m} = \hat{y} \cos\phi + \hat{q}(x) \times \hat{y} \sin\phi$, and ignoring terms which are non-zero only inside the Hubert wall (and hence do not contribute to non-local elasticity), one can rewrite (44) as

$$\mathcal{H}_0 \approx (J/2) \int_{\mathbf{r}} \left[\nabla\phi - \mathbf{q}(x)\right],^2 \quad (45)$$

which has the same form as (6). Thus, Hubert walls in non-centrosymmetric systems show long-range elasticity as well. All other conclusions made for Hubert walls and vortex walls transfer straightforwardly.

Liquid crystals. – Chiral nematic and smectic phases of liquid crystals exhibit a helical phase [34,35]. Their description is similar to that used in the non-centrosymmetric case, (44), provided $\mathbf{m}$ is replaced by the *director* $\mathbf{n}$, and J by the Frank constant. Further, in contrast to helimagnets, the direction of $\mathbf{q}$ is not fixed in space by anisotropy since chirality is introduced through the chirality of the molecules. DWs of the type described above will occur however as grain boundaries between phases with different $\mathbf{q}$-direction. A detailed discussion is beyond the scope of the present paper.

* * *

I thank R. D. Kamien, A. Rosch, B. Roostaei and C. Schüssler-Langeheine for useful discussions, V. L. Pokrovsky for a careful reading of the manuscript, and the Sino-French Center, Sun Yat-sen University Guangzhou for hospitality. This work has been supported through the Institutional Strategy of the University of Cologne within the German Excellence Initiative.

REFERENCES

[1] Haasen P., *Contemp. Phys.*, **18** (1977) 373.
[2] Fröhlich H., *Proc. R. Soc. London, Ser. A*, **223** (1954) 296.
[3] Hubert A. and Schäfer R., *Magnetic Domains: the Analysis of Magnetic Microstructures* (Springer) 2009.
[4] Kleemann W., *Annu. Rev. Mater. Sci.*, **37** (2007) 415.
[5] Parkin S. S. P., Hayashi M. and Thomas L., *Science*, **320** (2008) 190.
[6] Brazovskii S. and Nattermann T., *Adv. Phys.*, **53** (2004) 177.
[7] Li F., Nattermann T. and Pokrovsky V. L., *Phys. Rev. Lett.*, **108** (2012) 107203.
[8] Jensen J. and Mackintosh A., *Rare Earth Magnetism Structures and Excitations* (Oxford University Press, New York) 1991.
[9] Lang J. C., Lee D. R., Haskel D. and Srajer G., *J. Appl. Phys.*, **95** (2004) 6537.
[10] Pfleiderer C. *et al.*, *Nature*, **427** (2004) 227.
[11] Uchida M., Onose Y., Matsui Y. and Tokura Y., *Science*, **311** (2006) 359.
[12] Uchida M. *et al.*, *Phys. Rev. B*, **77** (2008) 184402.
[13] Kimura T. *et al.*, *Nat. Mater.*, **7** (2008) 291.
[14] Mostovoy M., *Phys. Rev. Lett.*, **96** (2006) 067601.
[15] Cheong S.-W. and Mostovoy M., *Nat. Mater.*, **6** (2007) 13.
[16] Chapon L. C. *et al.*, *Phys. Rev. Lett.*, **93** (2004) 177402.
[17] Kimura T. and Tokura Y., *J. Phys.: Condens. Matter*, **20** (2008) 434204.
[18] Talbayev D. *et al.*, *Phys. Rev. Lett.*, **101** (2008) 247601.
[19] Yamasaki Y. *et al.*, *Phys. Rev. Lett.*, **96** (2006) 207204.
[20] Chapon L. C. *et al.*, *Phys. Rev. B*, **83** (2011) 024409.
[21] Arima T., *J. Phys. Soc. Jpn.*, **80** (2011) 052001.
[22] Weschke E. *et al.*, *Phys. Rev. Lett.*, **93** (2004) 157204.
[23] Andrianov A. V., Kosarev D. I. and Beskrovnyi A. I., *Phys. Rev. B*, **62** (2000) 13844.
[24] Gennes P. D., *J. Phys. Radium*, **23** (1962).
[25] Joanny J. F. and de Gennes P. G., *J. Chem. Phys.*, **81** (1984) 552.
[26] Chaikin P. and Lubensky T., *Principles of Condensed Matter Physics* (Cambridge University Press) 1995.
[27] Noziere P., *Eur. Phys. J. B*, **24** (2001) 383.
[28] Schenck H., Pokrovsky V. L. and Nattermann T., arXiv:1308.0823 (2013).
[29] Hasenbusch M. and Pinn K., *J. Phys. A: Math. Gen.*, **30** (1997) 63.
[30] Janke W., *Phys. Lett. A*, **148** (1997) 306.
[31] Nattermann T., *Phys. Status Solidi (b)*, **132** (1985) 125.
[32] Grinstein G. and Ma S., *Phys. Rev. Lett.*, **49** (1982) 685.
[33] Nattermann T. *et al.*, *J. Phys. II*, **2** (1992) 1483.
[34] Kléman M., *Philos. Mag.*, **22** (1970) 739.
[35] Kléman M. and Lavrentovicht O. D., *Soft Matter Physics: An Introduction* (Springer, New York) 2003.